

## Altered biodistribution of deglycosylated extracellular vesicles through enhanced cellular uptake

Nao Nishida-Aoki<sup>a,b</sup>, Naomi Tominaga<sup>a,c</sup>, Nobuyoshi Kosaka<sup>a,d</sup> and Takahiro Ochiya<sup>a,d</sup>

<sup>a</sup>Division of Molecular and Cellular Medicine, National Cancer Center Research Institute, Tokyo, Japan; <sup>b</sup>Human Biology Division, Fred Hutchinson Cancer Research Center, Seattle, WA, USA; <sup>c</sup>Department of Biology, Massachusetts Institute of Technology, Cambridge, MA, USA; <sup>d</sup>Department of Molecular and Cellular Medicine, Institute of Medical Science, Tokyo Medical University, Tokyo, Japan

### ABSTRACT

Extracellular vesicles (EVs) from cancer are delivered both proximal and distal organs. EVs are highly glycosylated at the surface where EVs interact with cells and therefore has an impact on their properties and biological functions. Aberrant glycosylation in cancer is associated with cancer progression and metastasis. However, the biological function of glycosylation on the surface of EV is uncovered. We first demonstrated differential glycosylation profiles of EVs and their originated cells, and distinct glycosylation profiles in a brain-metastatic subline BMD2a from its parental human breast cancer cell line, MDA-MB-231-luc-D3H2LN by lectin blot. We then investigated the roles of surface glycoconjugates on EV uptake. N- and/or O-glycosylation removal of fluorescent-labelled BMD2a EVs enhanced cellular uptake to endothelial cells, suggesting that surface glycosylation has inhibitory effects on cellular uptake. Biodistribution of glycosylation-deprived BMD2a EVs administrated intravenously into mice was further analysed ex vivo using near-infrared lipophilic dye. EVs treated with O-deglycosylation enzymes enhanced the accumulation of EVs to the lungs after 24 h from the injection, while N-deglycosylation did not markedly alter biodistribution. As the lungs are first organs in which intravenous blood flows, we suggest that surface glycosylation of cancer-derived EVs avoid promiscuous adhesion to proximal tissues to be delivered to distant organs.

### ARTICLE HISTORY

Received 18 May 2019  
Revised 30 December 2019  
Accepted 2 January 2020

### KEYWORDS

Glycosylation; Sugar chain; glycan; Extracellular vesicles; Exosomes; Biodistribution

## Introduction

Extracellular vesicles (EVs), lipid bilayer vesicles secreted from cells, are widely recognized to stimulate cancer progression and metastasis. Cancer-derived EVs were delivered to both local and distant organs and incorporated into target cells to facilitate metastasis by conditioning pre-metastatic environment [1].


Aberrant glycosylation patterns are one of the hallmarks of cancer and contribute to the progressions of many types of cancers. In breast cancer, the correlation between glycosylation and metastasis has been discussed for 25 years (reviewed in [2]). Mucin and Galectins induce cell adhesion, migration, invasion and EMT. Especially, several reports have been shown a correlation between glycosylation and brain metastasis of breast cancer. Expression of Galectin-3 and Mucin-type O-glycans increased in the primary tumour and brain metastasis [3]. The  $\alpha$ 2,6-sialyltransferase ST6GALNAC5, expressed in both brain tissue and breast cancer cells, mediates the adhesions to brain endothelial cells and mediating cancer cells penetrating through the blood-brain barrier (BBB) [4]. Genomic analysis and the following DNA methylation

analysis identified highly-silenced GALNT9, an initiator of O-glycosylation, correlates with high brain metastasis [5]. Overall, aberrant carbohydrate structures contribute to malignancy in breast cancer.

The surface of EVs is enriched in glycoproteins and glycolipids. CD63, one of the major proteins on the surface of most EVs was shown to be highly glycosylated by ribophorin II (RPN2) in our previous work [6]. Protein glycosylation is mainly classified into N-linked and O-linked glycosylation based on atoms of amino acids covalently bind to glycosyl chains. However, the analysis of detailed structures of glycosyl chains is challenging because of their branched structures and heterogeneity. EVs have been shown to be enriched with glycosphingolipids by lipidomic analyses, although the importance of EV formation and secretion are under discussion [7].

Recent reviews summarized the potential roles of glycosylation in EV biogenesis, cellular recognition, and uptake of EVs [8–10]. Although glycosylation analysis suffers from technical limitations, several primary works reported the glycosylation repertoire of EVs. The glycosylation pattern of EV membrane is partially

**CONTACT** Takahiro Ochiya  [tochiya@tokyo-med.ac.jp](mailto:tochiya@tokyo-med.ac.jp); Nobuyoshi Kosaka  [nkosaka@tokyo-med.ac.jp](mailto:nkosaka@tokyo-med.ac.jp)  6-7-1, Nishi-shinjyuku, Shinjyuku-ku, Tokyo, 160-0023, Japan

 Supplemental data for this article can be accessed [here](#).

© 2020 The Author(s). Published by Informa UK Limited, trading as Taylor & Francis Group on behalf of The International Society for Extracellular Vesicles. This is an Open Access article distributed under the terms of the Creative Commons Attribution-NonCommercial License (<http://creativecommons.org/licenses/by-nc/4.0/>), which permits unrestricted non-commercial use, distribution, and reproduction in any medium, provided the original work is properly cited.

correlated but different from the cellular membrane in several cell types, such as T cells, melanoma, ovarian cancer, and colon cancer cells, suggesting selective loading of glycosyl chains into EVs. Gomes *et al.* compared glycosylation profiles of the total cell membrane and EVs of ovarian cancer cell lines using lectin array, demonstrating enriched sialic acids and several other glycosylations in EVs [11]. Escrevente *et al.*, also showed EVs from ovarian cancers are enriched in specific mannose- and sialic acid-containing glycoproteins [12], though sialic acid removal caused a small but non-significant increase in uptake. However, the importance of glycosylation of EVs for their biodistributions and functional contributions to cancer progression and metastasis remains unclear.

In the previous study, we have isolated a brain-metastatic breast cancer cell subline, BMD2a from a human triple-negative breast cancer cell line, MDA-MB-231-luc-D3H2LN [13]. Therefore, we investigated whether glycosylation of the surface of BMD2a EVs has any roles in EVs biodistribution. First, glycosylation patterns of cells and EVs from three breast cancer cell lines, BMD2a, MDA-MB-231-luc-D3H2LN, and MDA-MB-231-luc-D3H1 were profiled by lectin blots. Furthermore, the impacts of deprived glycosylation on EV uptakes of these cell lines and biodistribution of BMD2a were investigated.

## Experimental procedures

### Cell lines and reagents

Human triple-negative breast cancer cell lines, MDA-MB-231-luc-D3H1 and MDA-MB-231-luc-D3H2LN, were purchased from Xenogen (Alameda, CA, USA). A brain-metastatic breast cancer substrain, BMD2a, was established from MDA-MB-231-luc-D3H2LN in our previous work [13]. All breast cancer cell lines were maintained in RPMI1640 medium (GIBCO from Thermo Fisher Scientific, Waltham, MA, USA) supplemented with 10% FBS (v/v) (GIBCO) and 1% (v/v) antibiotic-antimycotic (GIBCO). MCF10A, an immortalized human breast epithelial cell line obtained from American Type Culture Collection, was maintained in MEGM BulletKit (Lonza, Basel, Switzerland). For the collection of EVs, the medium was replaced to advanced RPMI1640 (GIBCO) supplemented with 2 mM glutaMAX (GIBCO) and 1% (v/v) antibiotic-antimycotic (GIBCO). Human endothelial cell line (HUVECs) was purchased from Lonza and cultured in EGM-2 BulletKit (Lonza). All cells were cultured in a 5% CO<sub>2</sub> humidified incubator at 37°C.

For deglycosylation, N-Glycosidase F (*Flavobacterium meningosepticum*, recombinant from *E. coli*) was

purchased from Roche (Basel, Switzerland). O-Glycosidase & Neuraminidase Bundle (O-Glycosidase and  $\alpha$ 2-3,6,8 Neuraminidase) and Protein Deglycosylation Mix II (a mixture of Peptide-N-Glycosidase F: PNGase F, O-Glycosidase,  $\alpha$ 2-2,6,8,9 Neuraminidase A,  $\beta$ 1-4 Galactosidase S,  $\beta$ -N-acetylhexosaminidase<sub>F</sub>) were purchased from New England BioLabs (Ipswich, MA, USA). For lectin blots, biotinylated lectin sets 1 and 2 were purchased from Cosmo Bio (Tokyo, Japan). Streptavidin-conjugated with HRP was obtained from Cell Signalling Technology (Danvers, MA, USA).

### Isolation of EVs

Breast cancer cells cultured to 70–80% confluency were washed with PBS (-) twice and incubated with advanced RPMI1640 medium for 2 days. The conditioned media were centrifuged at 2000 × g, 10 min at 4°C and filtrated by 0.22  $\mu$ m filter to remove cell debris and large particles. EVs were collected by centrifuging the conditioned medium at 35,000 rpm for 70 min at 4°C using SW 41 Ti rotor (Beckman Coulter). The EVs were washed with filtrated PBS (-), and collected by resuspending to the remaining PBS in the centrifugation tube. The particle number of EVs with 200-fold dilutions was counted by NanoSight LM10 with NTA2.3 Analytical software (NanoSight) (Figure 1a, Supplementary Fig. 1), or at 100-fold dilutions with NanoSight NS-300 (Supplementary Fig. 2A, Supplementary Fig. 4B).

For fluorescent labelling, EVs were stained with a PKH67 Green Fluorescent Cell Linker Kit for General Cell Membrane Labelling (Sigma-Aldrich) for *in vitro* uptake assay, or DiR (Caliper Life Sciences) for biodistribution assay. Purified EVs were incubated with PKH67 at 2  $\mu$ M in PBS (-) for 5 min or DiR at 20  $\mu$ M in PBS (-) for 15 min at room temperature without light. The EVs were washed with PBS three times on a Vivacon 500 (100,000 MWCO) filter (Sartorius Stedim, Göttingen, Germany) to remove the unincorporated dye. The stained EVs were resuspended in PBS (-) and used for assays. The same volume of PBS (-) without EVs was treated simultaneously with the same control for non-vesicle controls.

### Lectin blot

Cells were lysed with by M-PER Mammalian Protein Extraction Reagent (ThermoFisher Scientific), and the supernatant was used as cell lysates. Protein concentration was measured by Bradford assay using bovine serum albumin (Pierce from Thermo Scientific) as a standard. EVs and cell lysates were denatured with sample buffer with 2-mercaptoethanol (Wako, Osaka,

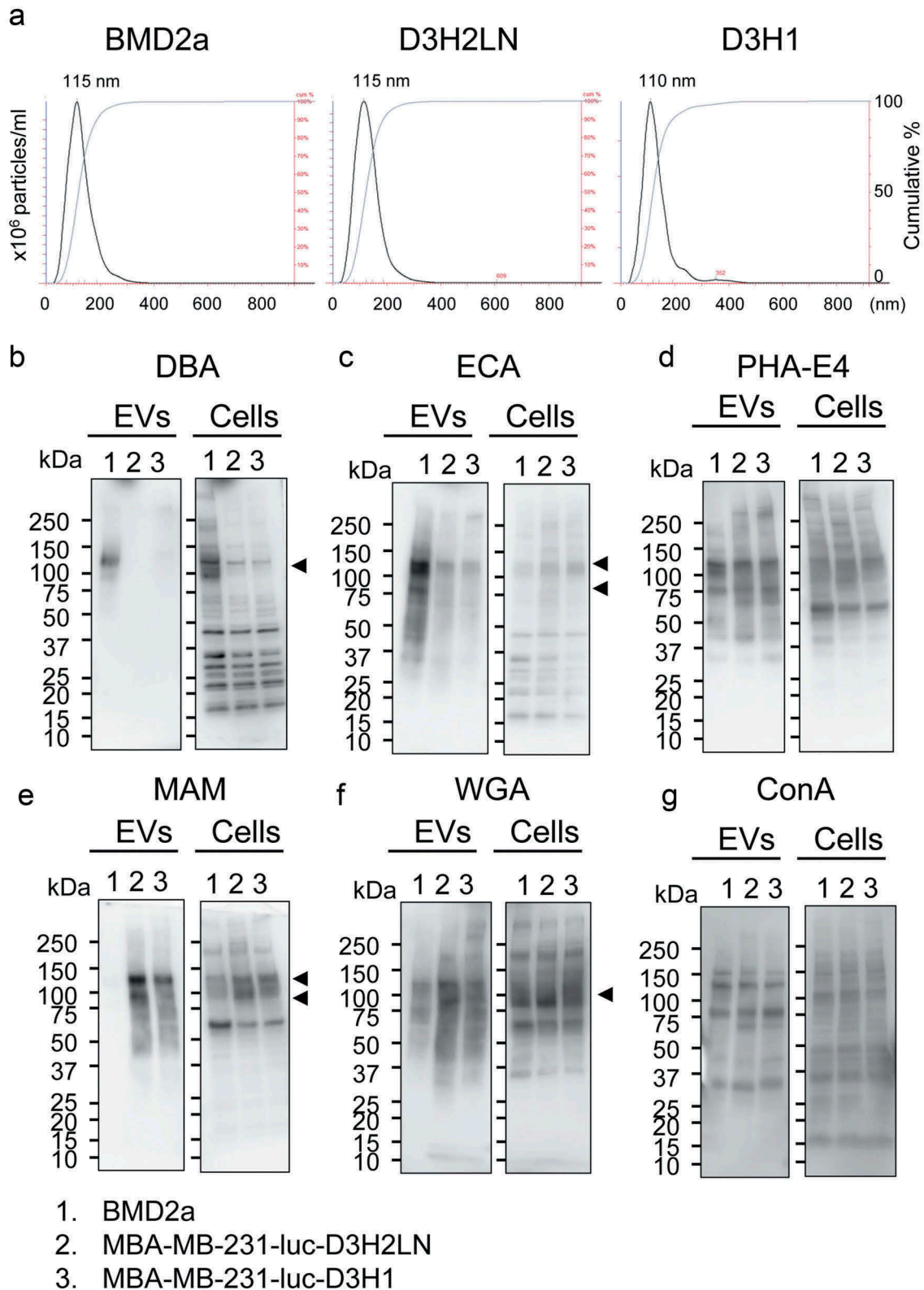


**Figure 1.** Glycosylation profiles of EVs and whole cells of breast cancer cell lines.

(a) The size distribution of EVs collected from breast cancer cell lines measured by the nanoparticle tracking system. EVs from brain-metastatic (BMD2a), lymph-node metastatic (MDA-MB-231-luc-D3H2LN, D3H2LN), and primary tumour-derived (MDA-MB-231-luc-D3H1, D3H1) breast cancer cell lines were isolated by ultracentrifugation and suspended into filtrated PBS. Data were obtained at 200-fold dilution. (b-g) Lectin blot profiles of cells and EVs of BMD2a, D3H2LN, and D3H1. EVs and cell lysates were separated by SDS-PAGE and transferred to nitrocellulose membrane. Then glycosyl chains were detected by biotinylated lectins followed by HRP-conjugated streptavidin. Lectins used for detections are: (b) DBA, (c) ECA, (d) PHA-E4, (e) MAM, (f) WGA, (g) ConA. Lectins and their specificities of glycosyl structures are summarized in [Table 1](#).

Japan) at 95°C, 5 min. Cell lysates were loaded 5 µg protein/well, and EVs were loaded at  $2.25 \times 10^9$  particles/well to run SDS-PAGE. Separated proteins were transferred to PVDF membrane. After blocked with Blocking One (Nacalai tesque, Kyoto, Japan), membranes were incubated with biotinylated lectins diluted in TBS-T at 20 µg/ml concentration, followed by probing with Streptavidin-HRP at 1:2000 dilution in TBS-T. The membrane was developed by Immunostar LD (Wako, Osaka, Japan), and the images were taken by CCD camera of ImageQuant LAS4000 (GE Healthcare, Chicago, IL, USA). A membrane without biotinylated lectins was processed at the same time to check non-specific binding of streptavidin-HRP.

### Deglycosylation enzyme treatment

Fluorescent-labelled EVs were treated with glycolytic enzymes (at least 2 unit/sample) at 37°C for 24 h. For Protein Deglycosylation Mix II, we followed the manufacturer's protocol. Samples supplemented with enzymes and buffer 2 were incubated at 25°C for 30 min, then incubated at 37°C for 24 h. The removal of glycans under this condition was confirmed by lectin blot (Supplementary Fig. 4A). The particle tracking analysis confirmed that the majority of EVs maintained their vesicle structures after the enzymatic digestion (Supplementary Fig. 4B).

### In vitro EV uptake assay

EVs derived from BMD2a, MDA-MB-231-D3H2LN, and MDA-MB-231-D3H1 were labelled with PKH67 green fluorescent dye, then treated with deglycosylation enzymes. HUVECs seeded on cover glass-bottom 8-well chambers ( $8 \times 10^4$  cells/well) were supplemented with EVs ( $1 \times 10^9$  particles/well). After 7 h, cells were washed and fixed with 4% paraformaldehyde. Nuclei were labelled with Prolong diamond with DAPI (ThermoFisher Scientific). Images were taken by confocal microscopy, Olympus FluoView FV10i (Olympus, Tokyo, Japan). Uptake of EVs was quantified based on fluorescence intensity using Fiji, the biological image analysis platform, and normalized by nucleic count within each image.

### Biodistribution of EVs in mice

The animal experiments in this study were performed in compliance with the guidelines of the Institute for Laboratory Animal Research, National Cancer Center Research Institute. Immunodeficient mice, C.B-17/Icr-scid/scid, female, at 5 to 6-week old were purchased from CLEA Japan (Tokyo, Japan) and Charles River Laboratories, Japan (Yokohama, Japan). DiR-stained

EVs treated with deglycosylation enzymes were injected intravenously from tail veins at the amount of EV equivalent to 5 µg protein/100 µl PBS per mice. After 24 h from the injection, the mice were sacrificed, and all organs were isolated to measure the fluorescence signal from the EVs trapped in the organs using IVIS Spectrum (PerkinElmer) with excitation/emission wavelength at 745 nm/800 nm. The radiant efficiency of the area of interest was evaluated by Living Image software accompanied with IVIS. To remove the background signal, the radiant efficiency from the organs from mice with no-EV control injected intravenously was measured and the average value subtracted from all the other signals. The relative amount of EVs accumulated in organs was calculated by dividing the radiant efficiency of the treated EVs by the average of non-treatment EVs. The amount of deglycosylation enzymes remained in enzyme-treated EVs was confirmed in advance to be not toxic to mice through intravascular administration.

## Results

### Glycosylation profiles of brain-metastatic breast cancer cells

EVs from brain-metastatic (BMD2a), lymph node-metastatic (MDA-MB-231-luc-D3H2LN: D3H2LN), and primary tumour-derived triple-negative breast cancer cell lines (MDA-MB-231-luc-D3H1: D3H1) were collected from the filtrated cultured-medium using ultracentrifugation. Particle-size distribution analyses confirmed that EVs from each strain have their distribution at 30–400 nm with peaks at 110–115 nm (Figure 1a). The protein amount incorporated into EV particle was similar among the EVs from the three cell lines (Supplementary Fig. 1). Then glycosylation profiles of EVs and whole cells of BMD2a, D3H2LN and D3H1 were analysed using lectin blot (Figure 1b–g). The specificities of each lectin to glycosylation structures are summarized in Table 1. Glycosylation patterns of D3H2LN and D3H1 were mostly similar, but BMD2a showed different patterns in both cellular and EVs. These results indicated that BMD2a drastically changed the glycosylation profiles during the repetitive selection process to obtain the ability to metastasis to the brain. Glycosylation recognised by *Dolichos biflorus* agglutinin (DBA), which has sugar specificity to N-acetylgalactosamine (GalNAc) and oligosaccharide specificity to GalNAcα1-3GalNAc, was enriched in both cells and EVs from BMD2a compared to D3H2LN and D3H1 (Figure 1b). Especially, glycosylation to proteins at a molecular weight at 120 kDa seemed to be enriched. The structure recognized by ECA (Galactose, GalNAc,



**Table 1.** Lectins used for detection of glycosylation of EVs and cells.

Lectins	Origin	Primary recognition sugars
DBA	<i>Dolichos biflorus</i>	D-GalNAc
ECA	<i>Erythrina cristagalli</i>	D-GalNAc, D-Gal, Lactose
PHA-E4	<i>Phaseolus vulgaris</i>	D-GalNAc
ConA	<i>Canavalia ensiformis</i>	$\alpha$ -D-Man, $\alpha$ -D-Glc
MAM	<i>Maackia amurensis</i>	Siaa2-3Gal
WGA	<i>Triticum vulgaris</i>	D-GlcNAc, Sialic acid

Lactose) was accumulated in EVs from BMD2a, but not in cells, suggesting that proteins with these glycosylations were accumulated into EVs (Figure 1c). Glycosylation recognized by PHA-E4, and high-mannose structures recognized by concanavalin A (ConA) was mostly similar among all three cell lines in both cells and EVs (Figure 1d,g). Glycosyl structures recognized by MAM and WGA were significantly decreased in EVs from BMD2a (Figure 1e,f). Since both MAM and WGA recognize sialic acids, the results indicate that EVs from BMD2a has less sialic acid on their surface. Additionally, glycosylation profiles of cells and EVs of the human mammary epithelial cell line, MCF10A, provided differential blot patterns from the cancer cells, indicating that EVs and cells from cancer cells are glycosylated differently from those from normal cells (Supplementary Fig. 2A, B). In all three cancer cell lines and MCF10A, different band patterns were observed between EVs and their producing cells. The results suggest that proteins and/or lipids with specific glycosylation are loaded into EVs during their formation, or glycosylation takes place on the surface of EVs although the mechanisms remain to be elucidated. These results indicate that the glycosylation patterns of BMD2a were altered from parental cell lines, and specific glycosylation patterns were accumulated in EVs compared to their cells of origin.

### Removal of surface glycans enhanced uptake of EVs *in vitro*

Next, we investigated whether the glycosyl modification at the surface of EVs has any physiological properties of EVs, such as EV uptake. EVs from BMD2a, D3H2LN, and D3H1 labelled with a lipophilic green fluorescent dye, PKH67, were treated with deglycosylation enzyme mix, which intensively removes both N- and O-linked glycans. For EV uptake experiment in the culture system, endothelial cells, which circulating EVs are supposed to first interact with to extravasate, were selected as a target of cancer-derived EVs. The deglycosylated or glycan-intact EVs were supplemented to human umbilical vein endothelial cell lines

(HUVECs), and after 7 h, the remaining EVs in the supernatants were washed out to observe EVs incorporated into cells under confocal microscope. The results from deglycosylated EVs clearly showed that the removal of glycosylation from EVs significantly stimulate the uptake of EVs from all three cell lines into HUVECs (Figure 2a, Supplementary Fig. 3A,B,C). These results suggest that glycosylation of EVs plays suppressive roles in EV uptake to HUVECs. Quantification of EV-derived fluorescence revealed that under untreated condition higher amount of BMD2a EVs was incorporated into HUVECs at 7 h than D3H2LN and D3H1 EVs, suggesting that the altered glycosylation profiles of BMD2a EVs observed in Figure 1 may contribute to the stimulated uptake into HUVECs (Supplementary Fig. 3A).

The impact of glycosylation subtypes on EV uptake was further analysed using EVs from BMD2a cells. PKH67-labelled EVs from BMD2a were treated by either N- or O-glycosylation degrading enzymes. Peptide-N-Glycosidase F (PNGase F) removes almost all N-linked glycans from glycoproteins. For O-deglycosylation, EVs were treated with a mixture of Neuraminidase and O-glycosidase because Neuraminidase removes sialic acids, which is a structural obstacle for O-glycosidase activities. Glycosylation patterns of EVs after treated with deglycosylation enzymes were analysed by lectin blots to confirm that glycosylations were removed (Supplementary Fig. 4A). Decreased molecular weight or decreased staining intensity was observed after deglycosylation, supporting that the activity of the deglycosylation enzymes. The particle size distribution and the number of BMD2a EVs after deglycosylation treatments remained mostly the same; therefore, EVs population compromised with vesicle structures after enzymatic treatment is ignorable (Supplementary Fig. 4B). The uptake of N- or O-glycosylation-deprived BMD2a EVs to HUVECs was tested in the same procedure as explained. N-, O-, or N- and O-glycosylation removal further increased BMD2a EVs uptake to HUVECs to similar levels (Figure 2b, Supplementary Fig. 3C). This result indicated that both N- and O- glycosylation on the surface of EVs have an inhibitory effect on EVs uptake *in vitro*.

### Surface glycans modulated biodistribution of EVs *in mice*

Next, we analysed whether removal of glycosylation has any impact on biodistribution in mice. EVs from BMD2a were labelled with a lipophilic near-infrared dye, DiR, which does not affect the biodistribution of EVs [14]. The stained EVs were treated with deglycosylation enzymes and administrated via tail vein into immune-compromised mice. After 24 h from

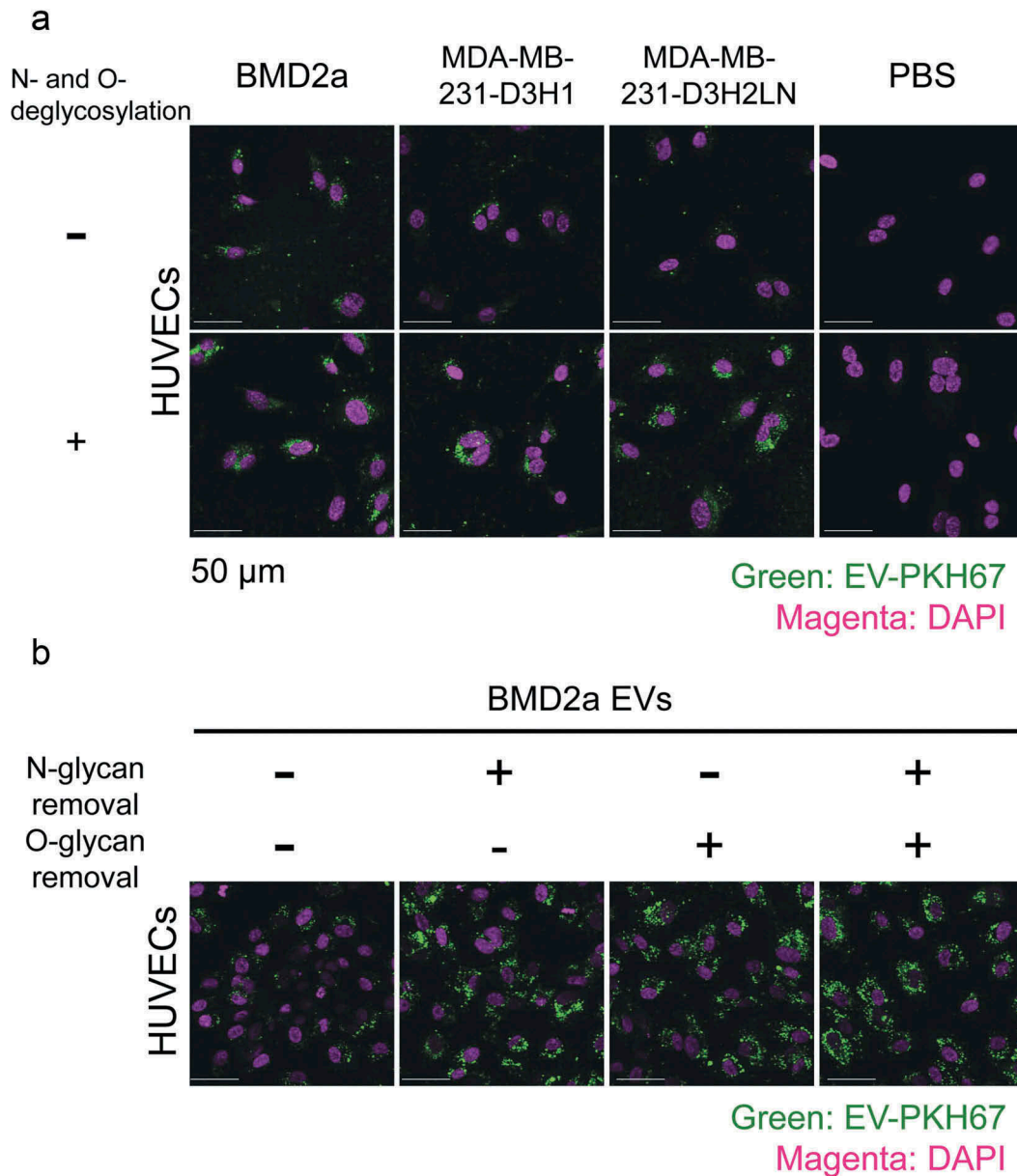


**Figure 2.** Microscopic images of deglycosylated EV uptake into HUVECs.

(a) Uptake of breast cancer EVs with or without extensive deglycosylation. EVs from BMD2a, D3H2LN, and D3H1 were labelled with a green fluorescent dye, PKH67, and treated with deglycosylation enzyme mix, which removes both N- and O-linked glycosyl chains. EV-free PBS was treated simultaneously as a background of dye staining. After 7 hrs from EVs supplemented to HUVECs, the remaining EVs were washed out. The cells were fixed, nuclear-labelled with DAPI, then observed under confocal microscopy. Scale bar: 50  $\mu$ m.

(b) Uptake of BMD2a EVs eliminated with N-linked or O-linked glycosylation. PKH67-labelled EVs from BMD2a were treated with N-glycosylation degradation enzymes, a mix of neuraminidase and O-glycosidase, or the deglycosylation enzyme mix which contain enzymes targeting both N-linked and O-linked glycosylation. Supplementation of EVs and observation were performed as above. Scale bar: 50  $\mu$ m.

the injection, mice were sacrificed to harvest organs, and the amount of EV accumulated to each organ was measured *ex vivo* through fluorescent intensity (Figure 3a). Treatment of enzymes removing O-linked glycans and the deglycosylation enzyme mix significantly increased the amount of EVs in the lungs, but not by N-linked deglycosylation (Figure 3b). The amount of EVs in the liver

remained at the same level among control and all deglycosylation enzyme treatments, and the deglycosylation enzyme mix treatment slightly increased EVs in the spleen. In the brain, EVs treated with O-linked deglycosylation enzymes showed a tendency of a slight increase of EVs, but not significant. Overall, these results proved that O-glycosylation has inhibitory roles of EVs uptake *in vivo*.

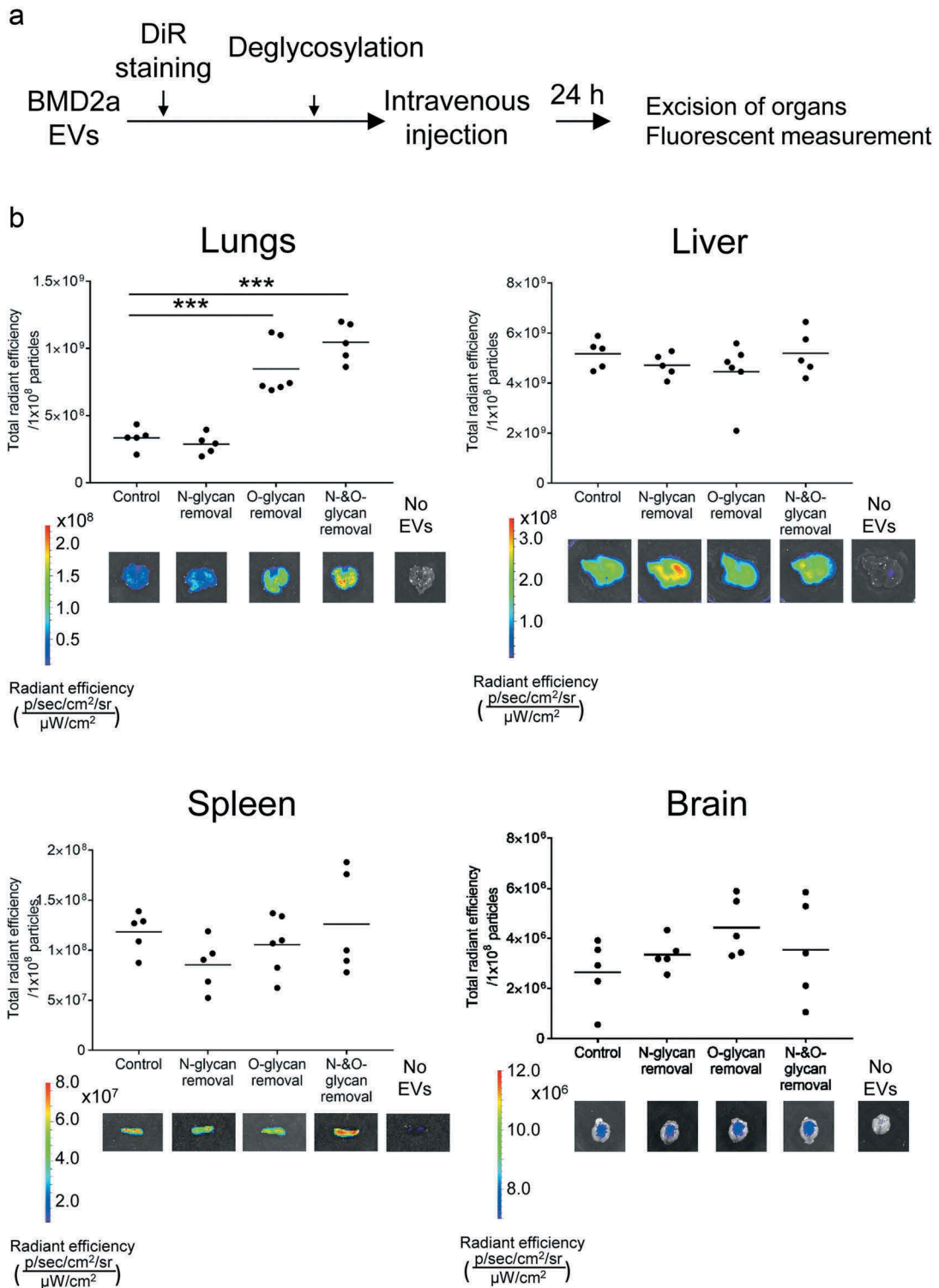


**Figure 3.** Biodistribution of deglycosylated EVs in mice after intravenous administration.

(a) Schematic of biodistribution observation of EVs treated with deglycosylation enzymes. BMD2a EVs were first labelled with a lipophilic near-infrared dye, then treated with deglycosylation enzymes. The EVs equivalent to 5  $\mu\text{g}$  protein per individual was administered into NSG female mice via tail vein. Mice were sacrificed, and organs were harvested after 24 h from the injection of EVs to measure fluorescent intensity under *in vivo* imaging system (IVIS).

(b) Amount of EVs accumulated into the lungs, liver, spleen and brain by fluorescent intensity after deglycosylation. The results from 5 to 6 individual mice are shown. Control indicates intact EVs with no glycosylation enzyme treatment. The representative organ images are shown at each enzyme treatment. The fluorescent intensities were normalized to per  $10^8$  particles of EVs. The bar indicated the average of each group. Statistical analysis was performed by unpaired two-tailed Student's t-test. \*\*\*:  $p < 0.001$ .

## Discussion

In this study, we described altered glycosylation patterns in brain-metastatic breast cancer cells and EVs, and demonstrated glycosylation of EVs has an inhibitory effect on EV uptake both *in vitro* and *in vivo*.

Glycosylation of tumour-EVs has been suggested being functionally important, but still, a few reports have been published. Recent work by Royo *et al.* reported altered biodistribution of EVs without terminal sialic acids in mice [15]. The authors radiolabelled EVs from the mouse liver progenitor cell line and observed the time-course distribution of the intravenously-administrated EVs under PET imaging. Neuraminidase-treated and non-treated EVs showed a similar distribution at the shorter time point, but treated EVs accumulated slightly higher at the lungs and the axillary nodes after 72 h. The data reported by Royo *et al.* provide evidence of the importance of glycosylation on the biodistribution of EVs. However, the authors only evaluated the effect of terminal sialic acids of glycoconjugates. Our results of EVs from human breast cancer cells also showed the accumulation of EVs to the lungs by O-linked glycan removal, although measured at 24 h after injection by lipophilic dye EV labelling (Figure 3b). We removed not only sialic acids but from the core of O-glycosylation, which possibly caused a larger impact on EV properties. Together, these results strongly support that O-glycosylation has an inhibitory effect on EV uptake. We suppose the accumulation of O-glycan-deprived EVs to the lungs was because EVs administrated in tail venous first flow into the lungs. Although mechanisms of selective EVs uptake remains uncovered, many pieces of evidence have shown that surface property of EVs is important for EV function as the surface is the place to first interact with recipient cells [16]. Removal of surface proteins alters the biodistribution of EVs in mice [17]. We assume glycosylation is preventing indiscriminate binding to proximate tissues to deliver EVs to distant organs, which are addressed by surface proteins such as integrins [18]. We suggest surface glycosylation is controlling EV delivery together with other surface proteins; less glycosylated EVs might be likely to be incorporated into the proximal tissues in an unspecific manner, and more glycosylated EVs will be delivered to the distant organs such as the brain through targeted delivery through surface proteins, which might correlate with malignancy of the tumours.

Another possibility of increased EV accumulation to the lungs by deglycosylation *in vivo* is that removal of glycosylation may help EVs to escape from innate immune systems. Lectins are expressed on immune cells, and different glycosylation patterns serve as an antigen to remove through phagocytosis. Shimoda

*et al.* recently suggested an interaction between sialic acids on EVs and cellular Sialic-acid-binding immunoglobulin (Ig)-like lectin (SIGLEC) is mediating accumulation of subcutaneously injected EVs into CD11b<sup>+</sup> cells in mouse lymph nodes (include dendritic cells and macrophages) [19]. The SCID mice we used for EV administration is immunodeficient, yet retain active innate immune systems, such as macrophages, dendritic cells, NK cells, and neutrophils. Experiments using mice with modified immune status are required to address this question.

Removal of N-linked glycans resulted in accelerated incorporation of EVs into HUVECs (Figure 2b) but did not alter the biodistribution of EVs in mice (Figure 3b). These results suggest the effect of glycosyl structure on EV uptake might be different depending on recipient cells. Although degradation of N-linked glycans did not alter the macro-perspective view of EV distribution, it may still stimulate regional uptake of EVs into specific cells in the mouse body, such as endothelial cells. We have performed EV detection by immunohistochemistry in formalin-fixed paraffin-embedded lung tissues to gain insights into the cell types that incorporated EVs, but the EVs were not detectable due to the technological limitation. More sensitive EV labelling with several experimental optimizations will answer the question.

We have previously shown EVs from BMD2a loosen brain–blood barrier (BBB) to help breast cancers to metastasize into the brain [13]. Altered glycosylation of BMD2a EVs observed in Figure 1b–g may contribute to EV delivery to the brain, by stimulated EV uptake to HUVECs together with by general inhibitory roles of glycosylation on incorporation. We observed tendencies but not a significant increase of EVs in the brain by O-glycan removal, which may be a result of counter-vailing enhanced adhesion to tissues with a decreased amount of EVs by being trapped at the lungs. The large variation observed in EVs without N- and O-glycans refrains us from making a clear conclusion (Figure 3b). As fluorescent intensity detected from the brain was much lower than other organs, EV labelling by DiR would not have enough detection power to analyse EVs went through BBB. Whether the altered glycosylation profile of EVs and cells of BMD2a has contributed to brain metastasis should be further investigated.

In conclusion, our findings underline the importance of glycosylation on EV uptake and biodistribution. We suggest surface glycosylation is controlling EV delivery by inhibiting non-specific binding to proximal tissues, to enable other surface proteins to target organs of their destination. This



knowledge will provide insights for roles of glycosylation on the physiological functions of EVs and practical application of EVs, such as drug delivery systems.

## Acknowledgments

We would like to thank Dr. Yusuke Yamamoto and Dr. Yusuke Yoshioka for suggestions and discussions over data. We would also like to thank Ms. Yurika Sawa for technical support. This work was supported in part by JSPS KAKENHI (Grant-in-Aid for Scientific Research (C)), Grant Number JP18K07253, and by Foundation for Promotion of Cancer Research in Japan. N.N.A was supported by a Grant-in-Aid for JSPS Fellows (No. 269202) and JSPS Overseas Research Fellowship (No. 416) from the Japan Society for the Promotion of Science. N.T. was supported by a Grant-in-Aid for JSPS Research Fellowships for Young Scientists (No. 5687), HOPE Research Fellowship from Foundation for Promotion of Cancer Research, and JSPS Overseas Research Fellowships (No.363).

## Contributions

Conceptualization, N.K. and T.O.; Methodology, N.N.A., N.T., and N.K.; Investigation, N.N.A., N.T., and N.K.; Writing – Original Draft, N.N.A.; Writing – Reviewing and Editing, N.N.A., N.T., N.K., and T.O.; Supervision, T.O.; Funding Acquisition, N.K. and T.O.

## Declaration of interest statement

N.N.A, N.T., N.K., and T.O. report no conflicts of interest.

## Funding

This work was supported by JSPS KAKENHI (Grant-in-Aid for Scientific Research (C)), Grant Number JP18K07253; Foundation for Promotion of Cancer Research in Japan. N.N.A was supported by a Grant-in-Aid for JSPS Fellows (No. 269202) and JSPS Overseas Research Fellowship (No. 416) from the Japan Society for the Promotion of Science. N.T. was supported by a Grant-in-Aid for JSPS Research Fellowships for Young Scientists (No. 5687), HOPE Research Fellowship from Foundation for Promotion of Cancer Research, and JSPS Overseas Research Fellowships (No.363).

## References

- [1] Becker A, Thakur BK, Weiss JM, *et al.* Extracellular vesicles in cancer: cell-to-cell mediators of metastasis. *Cancer Cell*. 2016;30:836–848.
- [2] Kölbl AC, Andergassen U, Jeschke U. The role of glycosylation in breast cancer metastasis and cancer control. *Front Oncol*. 2015;5:219. doi:10.3389/fonc.2015.00219.
- [3] Mayoral MA, Mayoral C, Meneses A, *et al.* Identification of galectin-3 and mucin-type O-glycans in breast cancer and its metastasis to brain. *Cancer Invest*. 2008;26:615–623.
- [4] Bos PD, Zhang XH-F, Nadal C, *et al.* Genes that mediate breast cancer metastasis to the brain. *Nature*. 2009;459:1005–1009.
- [5] Pangen RP, Channathodiyil P, Huen DS, *et al.* The GALNT9, BNC1 and CCDC8 genes are frequently epigenetically dysregulated in breast tumours that metastasise to the brain. *Clin Epigenetics*. 2015;7, 57. doi:10.1186/s13148-015-0089-x.
- [6] Tominaga N, Hagiwara K, Kosaka N, *et al.* RPN2-mediated glycosylation of tetraspanin CD63 regulates breast cancer cell malignancy. *Mol Cancer*. 2014;13:134.
- [7] Skotland T, Sandvig K, Llorente A. Lipids in exosomes: current knowledge and the way forward. *Prog Lipid Res*. 2017;66:30–41.
- [8] Williams C, Royo F, Aizpurua-Olaizola O, *et al.* Glycosylation of extracellular vesicles: current knowledge, tools and clinical perspectives. *J Extracell Vesicles*. 2018;7:1442985.
- [9] Gerlach JQ, Griffin MD. Getting to know the extracellular vesicle glycome. *Mol Biosyst*. 2016;12:1071–1081.
- [10] Costa J. Glycoconjugates from extracellular vesicles: structures, functions and emerging potential as cancer biomarkers. *Biochim Biophys Acta Rev Cancer*. 2017;1868:157–166.
- [11] Gomes J, Gomes-Alves P, Carvalho SB, *et al.* Extracellular vesicles from ovarian carcinoma cells display specific glycosignatures. *Biomolecules*. 2015;5:1741–1761.
- [12] Escrevente C, Keller S, Altevogt P, *et al.* Interaction and uptake of exosomes by ovarian cancer cells. *BMC Cancer*. 2011;11,108. doi:10.1186/1471-2407-11-108.
- [13] Tominaga N, Kosaka N, Ono M, *et al.* Brain metastatic cancer cells release microRNA-181c-containing extracellular vesicles capable of destructing blood-brain barrier. *Nat Commun*. 2015;6:6716.
- [14] Wiklander OPBB, Nordin JZ, O’Loughlin A, *et al.* Extracellular vesicle in vivo biodistribution is determined by cell source, route of administration and targeting. *J Extracell Vesicles*. 2015;4:1–13.
- [15] Royo F, Cossío U, Ruiz de Angulo A, *et al.* Modification of the glycosylation of extracellular vesicles alters their biodistribution in mice. *Nanoscale*. 2019;11:1531–1537.
- [16] Buzás EI, Tóth E, Sódar BW, *et al.* Molecular interactions at the surface of extracellular vesicles. *Semin Immunopathol*. 2018;40:453–464.
- [17] Charoenviriyakul C, Takahashi Y, Morishita M, *et al.* Role of extracellular vesicle surface proteins in the pharmacokinetics of extracellular vesicles. *Mol Pharm*. 2018;15:1073–1080.
- [18] Hoshino A, Costa-Silva B, Shen T-L, *et al.* Tumour exosome integrins determine organotropic metastasis. *Nature*. 2015;527:329–335.
- [19] Shimoda A, Tahara Y, Sawada S, *et al.* Glycan profiling analysis using evanescent-field fluorescence-assisted lectin array: importance of sugar recognition for cellular uptake of exosomes from mesenchymal stem cells. *Biochem Biophys Res Commun*. 2017;491:701–707.